PTCLab—a free and open source software for calculating phase transformation crystallography

X.-F. Gu[1], T. Furuhara[1], W.-Z. Zhang[2]

1. Institute for Materials Research, Tohoku University, Sendai 980-8577, Japan

2. Key Laboratory of Advanced Materials (MOE), School of Materials Science and Engineering, Tsinghua University, Beijing 100084, China

Synopsis - Introduce a free and open source program PTCLab for calculating phase transformation crystallography.

Abstract PTCLab (Phase Transformation Crystallography Lab) is a free and open source software to calculate the crystallographic features formed during a phase transformation, such as orientation relationship, interface orientation, interfacial structures etc. This program covers the crystallographic theories of martensitic and diffusional transformation and allows users to represent the results in stereo graphic projection. The crystallographic models treated in PTCLab include classical phenomenal theory of martensite crystallography (PTMC), double shear version of PTMC, invariant line model, O-lattice theory, O-line model, and recently developed 3-D NCS method, Edge-to-Edge matching model, variant selection analysis etc. In addition, a number of basic crystallographic calculations for single or multiple crystal structures could be done with the calculation pad. High quality composite stereographic projection and electron diffraction patterns can be also obtained by present application. PTCLab is written in python, runnable on cross platform and is distributed at https://sourceforge.net/projects/tclab/.

Keywords: Orientation relationship; Interface; Interfacial structure; Matensite crystallography; Precipitation crystallography; Variant selection

1. Introduction

Reproducible crystallographic features (such as morphologies, spatial distribution, orientation relationship (OR) etc.) are often observed during phase transformation and epitaxial growth. This preferred crystallography can often be rationalized with the help of geometry analysis, i.e. based on the fit/misfit analysis of lattice points or planes between two rigid lattices (Zhang & Weatherly, 2005; Zhang & Kelly, 2009). The geometry method is simple and takes lattice information sometimes orientation relationship as an input, and it can output rich information about crystallographic features (orientation relationship, interface orientation, interfacial structures etc.) and misfit strain distribution. As far as we know, there is no public integrated software for calculating phase transformation crystallography and illustrating the final results. Therefore, a free computer program named PTCLab (Phase Transformation Crystallography Lab) is developed.

2. PTCLab

PTCLab is a free and open-source software to calculate phase transformation crystallography for any crystal structures. It is developed with Python (Oliphant, 2007) with Matplotlib (Hunter, 2007) and Numpy (Van Der Walt *et al.*, 2011) libraries for publication quality plotting and numerical calculation, respectively. PTCLab supports multiple operating systems, and it can be downloaded from https://sourceforge.net/projects/tclab/ with a user manual.

2.1. Structure of PTCLab

The structure of PTCLab is shown in Figure 1. First of all, one needs to input the information of crystal structures. The symmetry information is not necessary, but it can be useful in different parts of the program, for example to reduce the crystallographic equivalent solutions or generate variants for a given orientation relationship. PTCLab supports different crystal systems with conventional and unconventional setting of space group. There are three method to input a crystal structure, one is to create the crystal structure by using PTCLab, second method is to input the structure by CIF file, and the third method is to obtain the structure directly from web database, such as the Crystallography Open Database (COD) (Grazulis *et al.*, 2009; Downs & Hall-Wallace, 2003), via the interface from PTCLab. For calculating phase transformation crystallography, minimum two crystal structures are needed.

After inputting crystal structures, one can plot pole figures, simulation diffraction patterns, and calculate transformation crystallography, etc. with PTCLab. The first two functions are useful for determining transformation crystallography associated with experimental data. Particularly, the function of diffraction pattern simulation can output not only overlapped diffraction patterns but also 2-D Kikuchi line/3-D Kikuchi line map for guiding conventional TEM operation.

The main function of PTCLab is to calculate transformation crystallography between dissimilar crystals. The calculation method is well documented in literatures (Zhang & Weatherly, 2005; Zhang & Kelly, 2009). The supported crystallographic models treated in PTCLab include classical phenomenal theory of martensite crystallography (PTMC) (Mackenzie & Bowles, 1954; Wechsler *et al.*, 1953), double shear version of PTMC (Ross & Crocker, 1970), O-lattice theory (Bollmann, 1982, 1970), invariant line model (Dahmen, 1982), O-line model (Zhang & Purdy, 1993; Qiu & Zhang, 2003; Gu & Zhang, 2014), near coincidence site (NCS) method (Liang & Reynolds, 1998) extended from structural ledge model (Rigsbee & Aaronson, 1979; Hall *et al.*, 1972), Edge-to-Edge matching model (Kelly & Zhang, 1999; Zhang & Kelly, 2009), and recent developed Good Matching Site (GMS) method (Yang & Zhang, 2012; Zhang, 2013) etc. For large misfit system, the coincidence site lattice (CSL)/displacement shift complete lattice (DSCL) method (Bollmann, 1982; Bonnet & Durand, 1975; Balluffi *et al.*, 1982, Ye & Zhang, 2002) is also included. Most methods except NCS method could output orientation relationship, interface normal, sometimes spacing and direction of interfacial defects. Although the NCS method needs OR as an input, it could be used to illustrate 3-D matching and find potential interfaces. PTCLab is developed for general application of transformation crystallography, and is not restricted to simple crystal structure such as FCC, BCC or HCP structure.
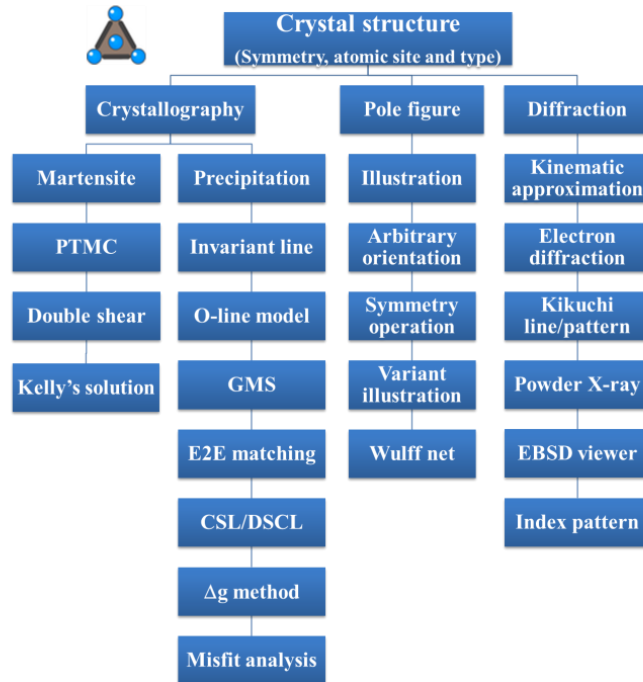

Figure 1 Structures of free software PTCLab.

2.2. Main interface of PTCLab

The main interface of PTCLab is shown in Figure 2, and it consists of menu (①in Figure 2), tool bar (②), item tree (③), and displayed panel (④). Different crystallographic models can be loaded from the "Calculation" menu. Tool bar offers system setting option and convenient operation of final results. All loaded the crystal structures are shown in item tree, and each item has three sub items for showing crystal structure, stereographic projection and electron diffraction pattern.
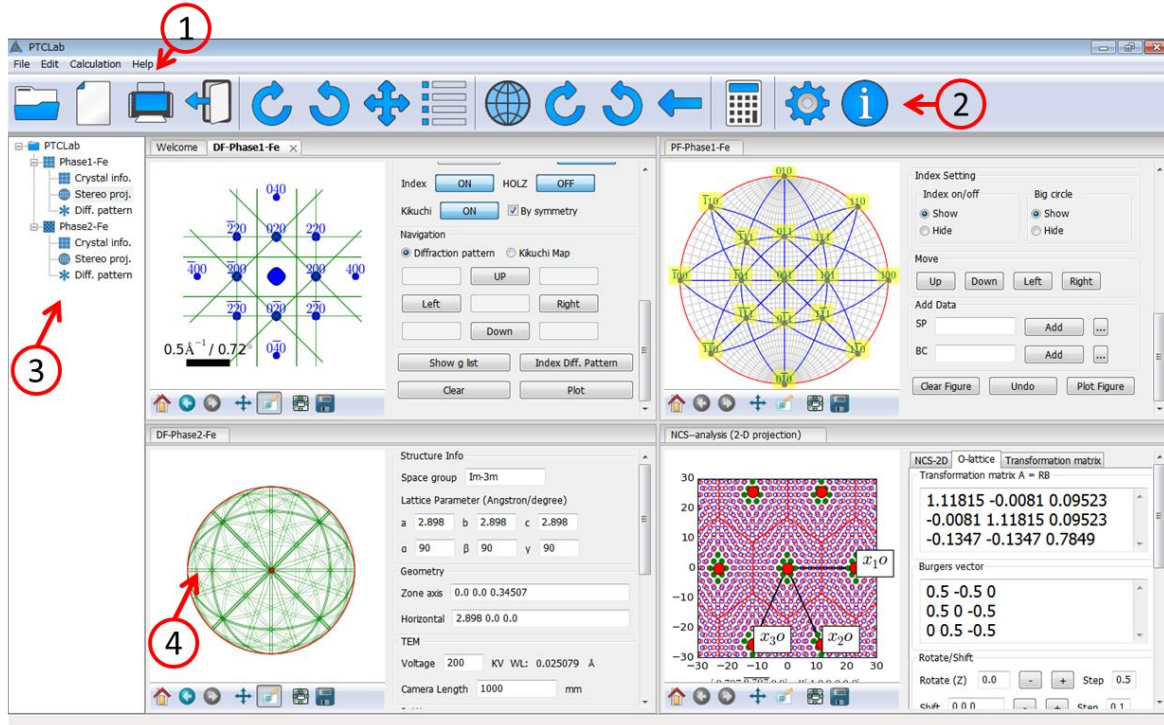

Figure 2 Main interface of PTCLab

3. Basic crystallography

3.1. Setting of orthogonal coordinate system

As shown in Figure 3a, a crystal coordinate system (e_1 // a, e_2 // b, e_3 // c) is defined by six lattice parameters, and this coordinate system is not straight for calculating the angles between directions or the length of a direction in a general crystal structure. Usually, an orthogonal coordinate system (x, y, z) is set up for calculation so that the vectors in crystal coordinate could be manipulated with knowledge in Cartesian coordinate system. Figure 3b-c shows two common settings In Figure 3b, the x axis is set to be parallel to e_1, and e_3 is fixed in the xz plane, while in Figure 3c, the z axis is set to be parallel to e_3, and e_1

is fixed in the **xz** plane. Though the selection of the different coordinate system conventions would not affect final results for angles and lengths, but cautions must be paid in some cases, especially when you apply Euler angle in Electron backscatter diffraction (EBSD) system, the alignment of the coordinate system is essential. When different coordinate system is selected, the Euler angle and the resulting orientation matrix would be different. In PTCLab, the convention of Figure 3b is adopted. The transformation of a vector in the crystal coordinate system v_c to orthogonal coordinate system v_o is related by

$$v_o = Sv_c \qquad (1)$$

where S is a structure matrix defined as

$$S = \begin{vmatrix} a & b\cos\gamma & c\cos\beta \\ 0 & b\sin\gamma & \dfrac{c}{\sin\gamma}(\cos\alpha - \cos\beta\cos\gamma) \\ 0 & 0 & \dfrac{V}{ab\sin\gamma} \end{vmatrix} \qquad (2a)$$

as function of the lattice parameters, and V is the volume of the crystal given by

$$V = abc\sqrt{1 + 2\cos\alpha\cos\beta\cos\gamma - (\cos\alpha)^2 - (\cos\beta)^2 - (\cos\gamma)^2} \qquad (2b)$$

In addition, the transformation of plane normal from a crystal coordinate system g_c to orthogonal coordinates system g_c is:

$$g_o = S^{-1\prime}g_c \qquad (3)$$

After setting of the orthogonal coordinate system, all calculation is carried out within this coordinate system, and final results of directions or plane normal are transformed to crystal coordinate system according to Equation (1) or (3), respectively.
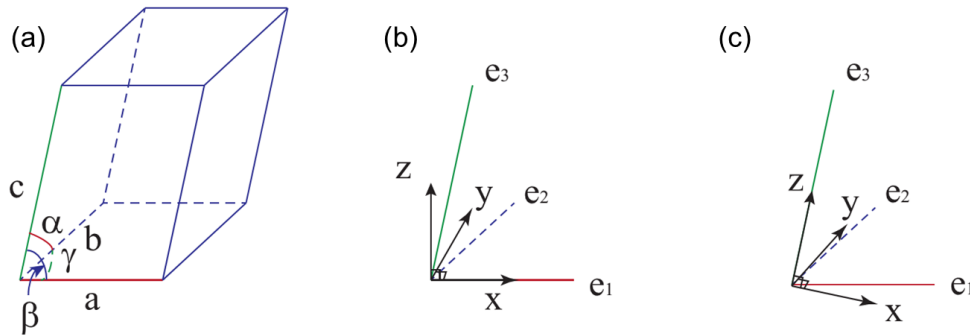

Figure 3 Coordinate system (a) Crystal defined by six lattice parameters (e_1 // **a**, e_2 // **b**, e_3 // **c**), (b) Definition of orthogonal coordinate system with **x** // e_1 and e_3 lying in **xz** plane. (c) Definition of orthogonal coordinate system with **z** // e_3 and e_1 lying in **xz** plane.

3.2. Orientation relationship and interface orientation

The orientation relationship describes the relative orientation between two crystals in 3D space. During phase transformations, reproducible ORs are often observed together with faceted/planar interfaces. The faceted interface could be described by a vector normal to the facet. The preferred interface usually corresponds to a local minimum of interfacial energy (Dai & Zhang, 2014). Therefore, the faceted interface is a key to understand the preferred crystallography during a phase transformation. A usual way to find the possible interfaces with minimum low energy or strain energy is to analyze the fit/misfit in all of the possible interfaces, and find the best matching interface as in various models showing in Figure 1.

The OR between two crystals could be described by several methods, such as miller indices, Euler angle, and axis/angle pairs. The straight way is to express the OR in miller indices. For example, the Nishiyama-Wassermann OR in FCC/BCC system is expressed as parallelism of low indexed planes $(111)_{fcc}$ // $(011)_{bcc}$ and parallelism of low indexed directions $[1\bar{1}0]_{fcc}$ // $[100]_{bcc}$. In some low symmetry system, such an expression would cause some misleading (Du *et al.*, 2016). The strictest way is to express the OR with the 3 by 3 orientation matrix $\mathbf{M}$ as used in PTCLab. The orientation matrix transforms a vector from one orthogonal coordinate system in one crystal or mechanical coordinate system (Section 3.1) to that in another crystal, such as from orthogonal coordinate system in matrix crystal $\mathbf{v}_m$ to that in product phase $\mathbf{v}_p$,

$$\mathbf{v}_p = \mathbf{M}\mathbf{v}_m \tag{4}$$

Therefore the orientation matrix is a rotation matrix with the determination equals to 1. The conversion of orientation matrix to three Euler angles is derived by G. Nolze with a sequence of rotation axes as ZXZ (Nolze, 2015). Systematic investigation of the ORs could be achieved by continuously varying Euler angles. In addition, the rotation axis/angle pair can be derived from orientation matrix as shown by Bollmann (Bollmann, 1982), where the rotation axis is expressed as

$$\mathbf{u} \text{ // } [m_{21}\text{-}m_{12}, m_{02} - m_{20}, m_{10}\text{-}m_{01}], \tag{5a}$$

and corresponding rotation angle can be expressed as:

$$\theta = \frac{m_{11} + m_{22} + m_{33} - 1}{2} \tag{5b}$$

where m_{ij} is the element of orientation matrix. Table 1 shows the examples of the common ORs in FCC/BCC system, such as Nishiyama-Wassermann (N-W) OR, Kurdjumov-Sachs (K-S) OR, Pitsch OR, with different expressions. The conversion between different expressions could be done by PTCLab, but the orientation matrix is a default input or output in various functions in PTCLab.

Table 1. Expressions of common orientation relationships in FCC/BCC systems.

OR	Miller indices	Euler angles	Rotational axis/angle pair

N-W	$(111)_{fcc} // (011)_{bcc}$ $[1\bar{1}0]_{fcc} // [100]_{bcc}$	(135.0, 9.7, 180.0)	$[0.201\ \overline{0.083}\ 0.976]$ / 46.0°
K-S	$(111)_{fcc} // (011)_{bcc}$ $[10\bar{1}]_{fcc} // [11\bar{1}]_{bcc}$	(114.2, 10.5, 204.2)	$[0.178\ \overline{0.178}\ 0.968\ ]$ / 42.8°
Pitsch	$(100)_{fcc} // (1\bar{1}0)_{bcc}$ $[011]_{fcc} // [111]_{bcc}$	(0.0, 9.7, 45.0)	$[\overline{0.201}\ 0.083\ \overline{0.976}\ ]$ / 46.0°

4. Application examples

In the following sections, only four examples are presented. As for the detailed examples and functions, please refer to the user manual.

4.1. Simulation of diffraction patterns

The OR between two crystals is usually determined by diffraction techniques such as transmission electron microscopy, EBSD etc. Therefore, the simulation or index the diffraction pattern is essential for studying phase transformation crystallography. PTCLab supports these functions. Figure 4 shows a simulated diffraction at N-W OR. Figure 4a and 4b are the electron diffraction pattern along $[1\bar{1}0]_{fcc}$ and $[100]_{bcc}$ zone axis, respectively, and Figure 4c is the superimposed diffraction pattern at N-W OR. PTCLab is capable of simulating the diffraction patterns of arbitrary crystals, i.e. not only in the high symmetry system as shown in Figure 4, but also in low symmetry system. Figure 5a shows another example of diffraction pattern from low symmetry crystal, i.e. monoclinic zirconia, together with Kikuchi lines. Recently, EBSD plays an important role in studying transformation crystallography (Miyamoto *et al.*, 2010; Miyamoto *et al.*, 2009; Humbert *et al.* 2011; Cayron *et al.*, 2006; Patapy *et al.*, 2013), thus the simulation of EBSD Kikuchi lines is performed in PTCLab. An example is shown in Figure 5b for the monoclinic zirconia as in Figure 5a (Patapy *et al.*, 2013). In addition to simulation of diffraction patterns and Kikuchi lines, PTCLab also offers a basic function to index diffraction pattern/Kikuchi line or EBSD Kikuchi line. The indexed OR is expressed in Euler angles which is convenient for further calculation.
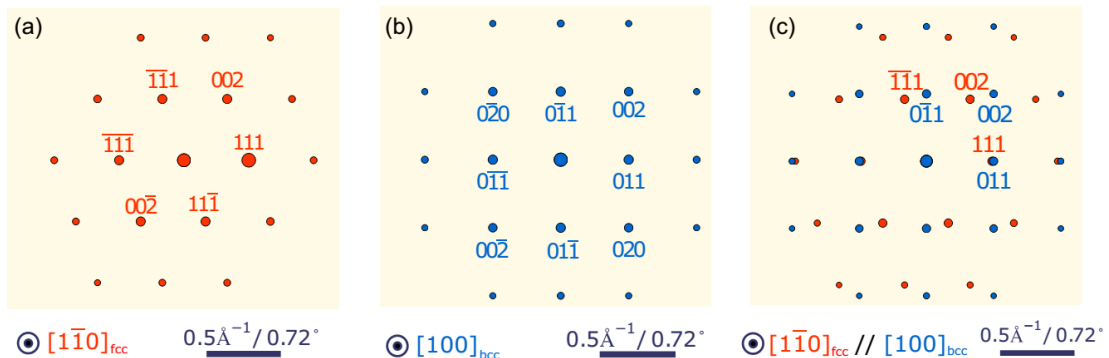
Figure 4 Simulated diffraction patterns in FCC/BCC systems by PTCLab. (a) Diffraction pattern along [1$\bar{1}$0] in FCC lattice, (b) Diffraction pattern along [100] in BCC lattice, (c) Superimposed diffraction patterns at N-W OR. Red dots are spots from FCC crystal, while blue dots are from BCC crystal.
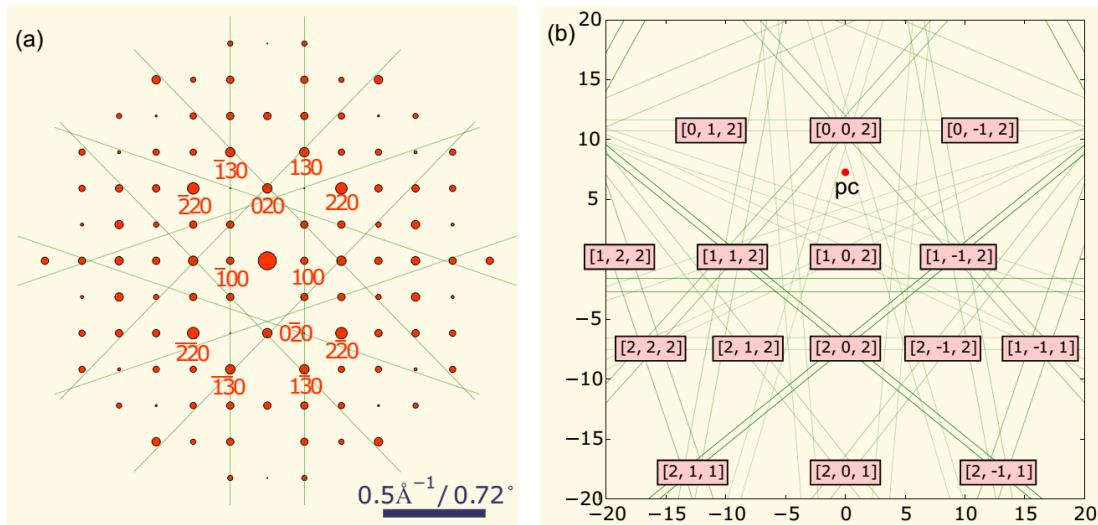

Figure 5 Simulated diffraction patterns for monoclinic zirconia crystal. (a) Diffraction pattern and Kikuchi lines along [002] direction, (b) EBSD Kikuchi pattern for the sample with orientation of (0,0,0) at 20 KV with sample tilt angle of 70°, where the labelled indices are the direction of plane intersections and 'pc' stands for pattern centre.

4.2. Misfit analysis and misfit dislocation

As mentioned before, the basis of the geometrical models for transformation crystallography is based on fit/misfit analysis of the atoms from two crystals. Suppose two crystals are interpenetrated with each other, the closest distance between two atoms from two crystals are defined as misfit value. The geometrical model requires the misfit value to reach their minimum at the interface or growth direction, for example, if the misfit value along one direction is zero, then this direction is an invariant line (Dahmen, 1982). The NCS method is based on the misfit distribution, and the atoms with misfit smaller than certain value (15%|$\mathbf{b}$|, $\mathbf{b}$ is Burgers vector) is defined as NCS point (Liang & Reynolds, 1998) or GMS point (Yang & Zhang, 2012; Zhang, 2013). Figure 6a shows the NCS distribution in (111)$_f$//(011)$_b$ at N-W orientation relationship (OR). The advantage of NCS method is easy to use and without input of lattice correspondence (Liang & Reynolds, 1998; Furuhara et $al.$, 2002), but the disadvantage is that it is unable to quantitatively analyse the match/mismatch between two crystals. In contrast, the quantitative method is O-lattice theory, though it is not straight as NCS method. These two complementary methods

are all included in PTCLab. As for the case in Figure 6a, the O-lattice and O-cell wall are plotted in Figure 6b by inputting the Burgers vectors $<1\bar{1}0>/2$ on $(111)_f$ plane. The O-cell wall is the worst matching place thus it is the location of the dislocations. The solution of the O-cell wall is based on the solution of Bollmann's equation (Zhang, 2005). Apparently, O-lattice is the center of the NCS points or GMS points. When the OR varies, the dislocation structure and the distribution of good matching atoms change accordingly. For example, when the OR deviates 3° from N-W OR around plane $(111)_f//(011)_b$, the O-lattice distribution and dislocation structure is shown in Figure 6c. The quantitative result of the dislocation line direction and spacing can be output from PTCLab. In some singular cases, the O-lattice does not exist, but the GMS point can also be defined and the dislocation structure can be also defined by GMS method (Zhang, 2013). PTCLab supports the treatment of these special cases.

4.3. Martensite crystallography

Phenomenal theory of martensite crystallography (PTMC) (Mackenzie & Bowles, 1954; Wechsler *et al.*, 1953) is recognized as the milestone in studying phase transformation crystallography (Wayman, 1964). The development of precipitation crystallography, such as O-line solution (Qiu & Zhang, 2003; Gu & Zhang, 2010), is benefit from its matrix solution. The developed double shear version of PTMC (Ross & Crocker, 1970) and a special solution proposed by Kelly (Kelly, 1992) are also included in PTCLab in addition to PTMC. Here, we take the classical PTMC theory as an example. The inputted crystal structures in PTCLab are the same as in the book (Bhadeshia, 2001), i.e FCC structure and BCC structure with lattice parameters as $a_f = 3.56$Å $a_b = 2.8598$ Å, respectively. The calculated result by PTCLab is partly shown in Table 2. The solutions are consistent with previous results (Bhadeshia, 2001). There are four solutions in total. For each solution, the calculated crystal directions or planes are expressed in both FCC and BCC crystals so that one can distinguish between different solutions. The habit plane (HP) in FCC are crystallographic equivalent for four solutions are located on an eclipse curve as shown in Figure 7 (Gu & Zhang, 2011), however, the expression in BCC lattice is different. Therefore, four solutions can be divided into two categories, i.e. solution 1 and solution 4 are crystallographically equivalent while solution 2 and 3 are crystallographically equivalent solution. For a twining martensite, the martensite consists of the variants of these two categories. The volume fraction of the twining could be calculated from the magnitude of lattice invariant shear m_1 (Bhadeshia, 2001), and the twin ratio is $0.401/0.265 = 1.513 : 1$, i.e. the volume fraction of smaller m_1 is around 60%. In summary, PTCLab could output complete crystallographic data for both martensite crystallography and precipitation crystallography, which is ready for comparison with the experimental data.
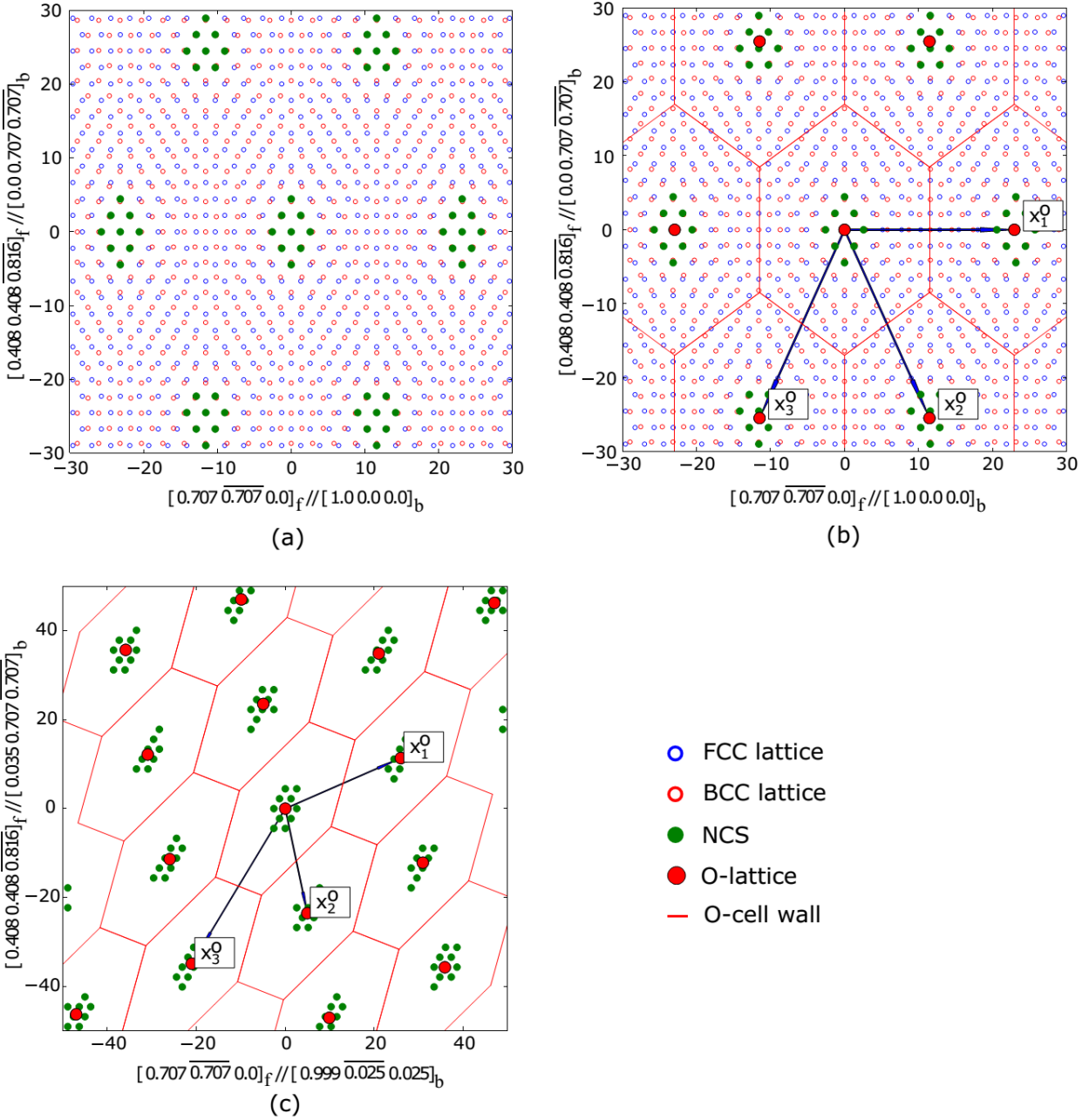
Figure 6 Dislocation on the interface, (a) N-W OR ($(111)_f//(011)_b$, $[1\bar{1}0]_f//[100]_b$), (b) O-lattice and O-cell wall calculated by O-lattice theory for N-W OR. Three principal O-lattice vectors $\mathbf{x}^O_i$ (i = 1, 2, 3) correspond to the Burgers vector $<1\bar{1}0>/2$, $<10\bar{1}>/2$ and $<01\bar{1}>/2$, respectively. (c) O-lattice and O-cell wall for the OR between two lattices deviates 3° from N-W OR.

Table 2. Transformation crystallography for martensite calculated by PTCLab, IL is invariant line direction, IL* is invariant normal direction, RB is the transformation matrix, HP is the habit plane, m_1 is the magnitude of lattice invariant shear and m_2 is the magnitude of macroscopic shape change. OR is expressed in miller index in the last two columns.

Solution 1

IL(fcc)	-0.671	IL(bcc)	-0.792
	0.315		-0.286
	0.671		0.539
IL*(fcc)	0.539	IL*(bcc)	-0.067
	0.647		0.738
	0.539		0.671
RB	1.107	-0.116	0.161
	0.105	1.129	0.044
	-0.233	-0.040	0.786
HP(fcc)	-0.571	HP(bcc)	0.097
	-0.797		-0.931
	-0.197		-0.351
m_1	0.401	m_2	0.223

OR	fcc	bcc	Angle
Plane	1 1 1	0. 1. 1.	0.436
Dir.	1 0 -1	1. 1. -1.	3.285

Solution 2

IL(fcc)	-0.671	IL(bcc)	-0.286
	-0.315		-0.792
	0.671		0.539
IL*(fcc)	0.539	IL*(bcc)	-0.067
	0.647		0.738
	0.539		0.671
RB	1.125	-0.040	0.107
	0.024	1.129	0.085
	-0.154	-0.116	0.792
HP(fcc)	-0.197	HP(bcc)	0.419
	-0.797		-0.609
	-0.571		-0.673
m_1	0.265	m_2	-0.223

OR	fcc	bccc	Angle
Plane	1 1 1	0. 1. 1.	0.436
Dir.	1 -1 0	2. 0. 0.	2.039

Solution 3

IL(fcc)	-0.671	IL(bcc)	-0.792
	0.315		-0.286
	0.671		0.539
IL*(fcc)	0.539	IL*(bcc)	0.738
	-0.647		-0.067
	0.539		0.671
RB	1.125	0.040	0.107
	-0.024	1.129	-0.085
	-0.154	0.116	0.792
HP(fcc)	-0.197	HP(bcc)	-0.609
	0.797		0.419
	-0.571		-0.673
m_1	0.265	m_2	-0.223

OR	fcc	bcc	Angle
Plane	1 -1 1	1. 0. 1.	0.4364
Dir.	1 1 0	0. 2. 0.	2.039

Solution 4

IL(fcc)	-0.671	IL(bcc)	-0.286
	-0.315		-0.792
	0.671		0.539
IL*(fcc)	0.539	IL*(bcc)	0.738
	-0.647		-0.067
	0.539		0.671
RB	1.107	0.116	0.161
	-0.105	1.129	-0.044
	-0.233	0.040	0.786
HP(fcc)	-0.571	HP(bcc)	-0.931
	0.797		0.097
	-0.197		-0.351
m_1	0.401	m_2	0.223

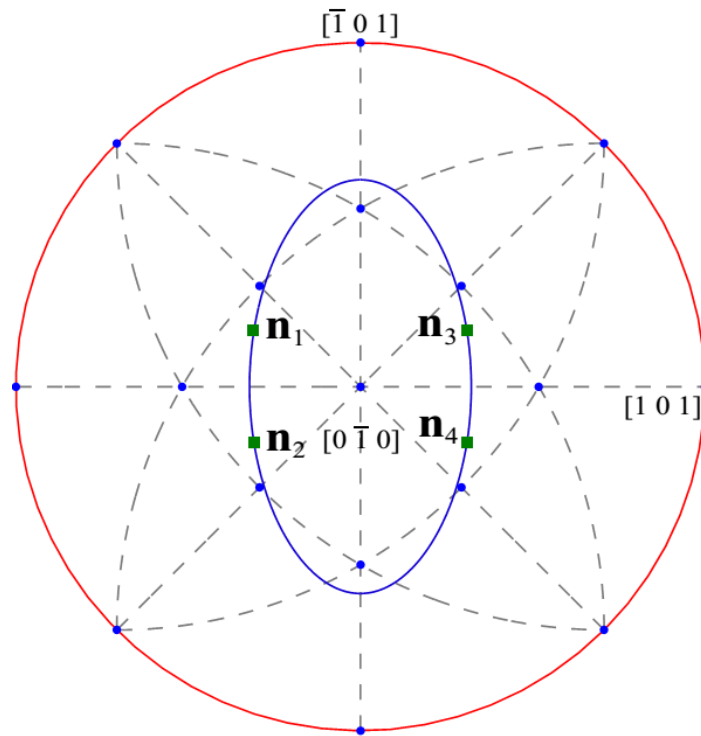| OR	fcc	bcc	Angle
Plane	1 -1 1	1. 0. 1.	0.436
Dir.	1 0 -1	1. 1. -1.	3.285

Figure 7 Stereographic projection of the habit normal for the solutions in Table 1.

4.4. Variants due to crystal symmetry

Due to the symmetry of the matrix, the transformed products may have crystallographically equivalent solutions which are called variants. The boundaries between variants could be served as an effective boundary to strengthen the material. The number of variants depend on the symmetry of matrix and product phase and OR (Humbert *et al.* 1992). PTCLab supports most conventional or unconventional setting of the space group, the symmetry operation can be generated by PTCLab, and thus the variant number and crystallography feature of each variant can be outputted by PTCLab. Furthermore, the variants could be classified by PTCLab according to different criterion, such as Bain group, Close Packed direction group, Close Packed plane group etc. The distribution of the variants could be shown in a stereographic projection by PTCLab as Figure 8. Figure 8 shows 24 BCC variants at K-S OR in FCC/BCC system, and it could be seen from the figure that the distribution of the variants reflects the symmetry of the parent FCC crystal. Such a variant distribution can be manipulated by changing OR via Euler angles, thus it could be applied in fitting OR from experimental results (Nolze, 2006).

With the crystallographic data of each variant, PTCLab offers a calculation of variant selection based on the model proposed by Furuhara et al (Furuhara *et al.*, 2008). The variant selection rules executed in

PTCLab include (1) minimization the angle between the shape strain direction or slip direction and specific plane, (2) minimization the angle between specific planes. These rules are also applicable to variant selection along grain boundary as in original work (Furuhara *et al.*, 2008).
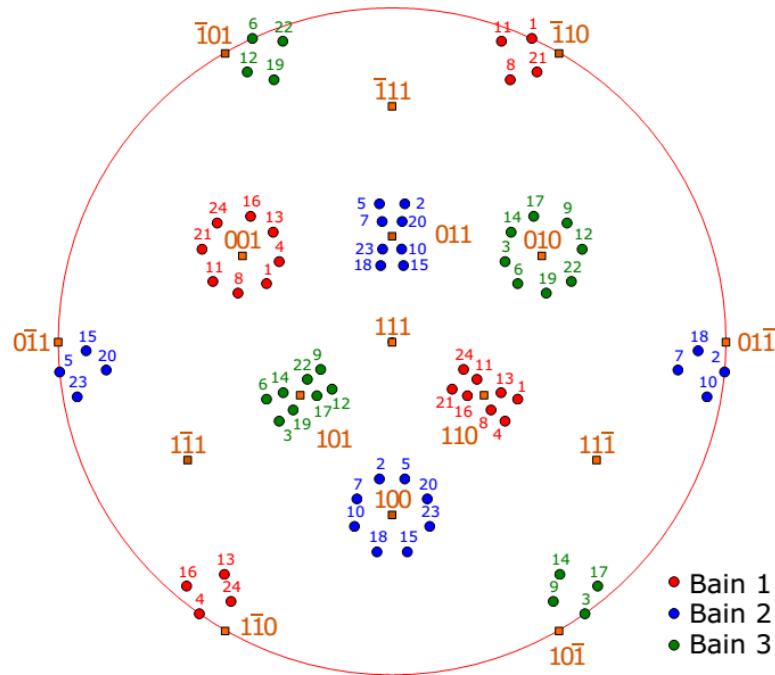

Figure 8 $[111]_f$ stereographic projection of $<001>_b$ of 24 BCC variants at K-S OR ($(111)_f//(011)_b$, $[10\bar{1}]_f//[11\bar{1}]_b$). Different colour shows different Bain group, and filled circles are from bcc lattices, while filled squares are from FCC lattice. The number indicates different BCC variants.

5.　　Future developments

Further version will cover following aspects. Firstly, function to fit crystallographic feature from EBSD data and to analyse the variant distribution of product phases. Secondly, function to search crystal structures fulfilling certain crystallographic criterion (such as small misfit) from COD database, which could be useful for alloy development by crystallography engineering.

6.　　Conclusion

A free and open-source software PTCLab for calculating phase transformation crystallography in arbitrary alloy system is released at https://sourceforge.net/projects/tclab/. The software is written in python, runnable on cross platform. It supports most geometrical models for transformation crystallography with quantitative outputs (orientation relationship, dislocation spacing, growth direction

etc.). In addition, the simulation of diffraction patterns/Kikuchi lines and quality plot of stereo-graphic projection are also included. Although our understanding of transformation crystallography is still in many ways imperfect, the development of the transformation crystallography is impressive. PTCLab could be helpful in the research of transformation crystallography.

Figure 1   Structures of free software PTCLab.

Figure 2   Main interface of PTCLab.

Figure 3   Coordinate system (a) Crystal defined by six lattice parameters ($\mathbf{e}_1$ // $\mathbf{a}$, $\mathbf{e}_2$ // $\mathbf{b}$, $\mathbf{e}_3$ // $\mathbf{c}$), (b) Definition of orthogonal coordinate system with $\mathbf{x}$ // $\mathbf{e}_1$ and $\mathbf{e}_3$ lying in $\mathbf{xz}$ plane. (c) Definition of orthogonal coordinate system with $\mathbf{z}$ // $\mathbf{e}_3$ and $\mathbf{e}_1$ lying in $\mathbf{xz}$ plane.

Figure 4   Simulated diffraction patterns in FCC/BCC systems by PTCLab. (a) Diffraction pattern along $[1\bar{1}0]$ in FCC lattice, (b) Diffraction pattern along [100] in BCC lattice, (c) Superimposed diffraction patterns at N-W OR. Red dots are spots from FCC crystal, while blue dots are from BCC crystal.

Figure 5   Simulated diffraction patterns for monoclinic zirconia crystal. (a) Diffraction pattern and Kikuchi lines along [002] direction, (b) EBSD Kikuchi pattern for the sample with orientation of (0,0,0) at 20 KV with sample tilt angle of 70°, where the labelled indices are the direction of plane intersections and 'pc' stands for pattern centre.

Figure 6   Dislocation on the interface, (a) N-W OR ($(111)_f$//$(011)_b$, $[1\bar{1}0]_f$//$[100]_b$), (b) O-lattice and O-cell wall calculated by O-lattice theory for N-W OR. Three principal O-lattice vectors $\mathbf{x}^O_i$ ($i = 1, 2, 3$) correspond to the Burgers vector $<1\bar{1}0>/2$, $<10\bar{1}>/2$ and $<01\bar{1}>/2$, respectively. (c) O-lattice and O-cell wall for 3° from N-W OR.

Figure 7   Stereographic projection of the habit normal for the solutions in Table 1.

Figure 8 $[111]_f$ stereographic projection of $<001>_b$ of 24 BCC variants at K-S OR ($(111)_f$//$(011)_b$, $[10\bar{1}]_f$//$[11\bar{1}]_b$). Different colour shows different Bain group. Different colour shows different Bain group, and filled circles are from bcc lattices, while filled squares are from FCC lattice.

Table 1   Expressions of common orientation relationships in FCC/BCC systems.

Table 2   Transformation crystallography for martensite calculated by PTCLab, IL is invariant line direction, IL* is invariant normal direction, RB is the transformation matrix, HP is the habit plane, m_1 is the magnitude of lattice invariant shear and m_2 is the magnitude of macroscopic shape change. OR is expressed in miller index in the last two columns.

References

Balluffi R. W., Brokman A., & King A. H. (1982). Acta Metall. **30**, 1453-70.

Bhadeshia, H. K. D. H. (2001). *Worked examples in the Geometry of Crystals*. London: Institute of
    Materials.

Bollmann, W. (1970). *Crystal defects and crystalline interfaces*. Berlin: Springer.

Bollmann, W. (1982). *Crystal lattices, interfaces, matrices*. Geneva: Bollmann.

Bonnet R. & Durand F. (1975). Philos. Mag. , **32**, 997-1006.

Cayron, C., Artaud, B. & Briottet, L. (2006). *Mater.Charact.* **57**, 386-401.

Dahmen, U. (1982). *Acta Metall.***30**, 63-73.

Dai, F.-Z. & Zhang, W.-Z. (2014). *Acta Metall Sin* **50**, 1123-1127.

Downs, R. T. & Hall-Wallace, M. (2003). *American Mineralogist* **88**, 247-250.

Du, J., Zhang, W.-Z., Dai, F.-Z. & Shi, Z.-Z. (2016). *J. Appl. Cryst.***49**, 40-46.

Furuhara, T., Kawata, H., Morito, S., Miyamoto, G. & Maki, T. (2008). *Metall. Mater.Trans.* **39A**, 1003-
    1013.

Furuhara, T., Oishi, K. & Maki, T. (2002). *Metall. Mater.Trans.* **33A**, 2327-2335.

Grazulis, S., Chateigner, D., Downs, R. T., Yokochi, A. F. T., Quiros, M., Lutterotti, L., Manakova, E., Butkus,
    J., Moeck, P. & Le Bail, A. (2009). *J. Appl. Cryst.***42**, 726-729.

Gu, X.- F. & Zhang, W.-Z. (2010). *Philos. Mag.* **90**, 4503 - 4527.

Gu, X.-F. & Zhang, W.-Z. (2011). *Acta Metall. sinica* **47**, 241-245.

Gu, X.-F. & Zhang, W.-Z. (2014). *Metall. Mater.Trans.* **45A**, 1855-1865.

Hall, M. G., Aaronson, H. I. & Kinsma, K. R. (1972). *Surf.Sci.* **31**, 257-274.

Humbert, M., Blaineau, P., Germain, L. & Gey, N. (2011) . *Scripta Mater.* **64**, 114-117.

Humbert, M., Wagner, F., & Esling, C. (1992). *J. Appl. Cryst.* **25**, 724-730.

Hunter, J. D. (2007). *Comput. Sci. Eng.* **9**, 90-95.

Kelly, P. M. (1992). *Mater.Trans.* **33**, 235-242.

Kelly, P. M. & Zhang, M. X. (1999). *Mater. Forum* **23**, 41-62.

Liang, Q. & Reynolds, W. T., Jr. (1998). *Metall. Mater.Trans.* **29A**, 2059-2072.

Mackenzie, J. K. & Bowles, J. S. (1954). *Acta Metall.* **2**, 138-147.

Miyamoto, G., Iwata, N., Takayama, N. & Furuhara, T. (2010). *Acta Mater.***58**, 6393-6403.

Miyamoto, G., Takayama, N. & Furuhara, T. (2009). *Scripta Mater.* **60**, 1113-1116.

Nolze, G. (2006). *Cryst. Res. Technol.* **41**, 72-77.

Nolze, G. (2015). *Cryst. Res. Technol.* **50**, 188-201.

Oliphant, T. E. (2007). *Comput. Sci. Eng.* **9**, 10-20.

Patapy, C., Huger, M., Guinebretière, R., Gey, N., Humbert, M., Hazotte, A. & Chotard, T. (2013). *J. Eur.
    Ceram. Soc.* **33**, 259-268.

Qiu, D. & Zhang, W.-Z. (2003). *Philos.Mag.***83**, 3093-3116.

Rigsbee, J. M. & Aaronson, H. I. (1979). *Acta Metall。* **27**, 351-363.

Ross, N. D. H. & Crocker, A. G. (1970). *Acta Metall.* **18**, 405-418.

Van Der Walt, S., Colbert, S. C. & Varoquaux, G. (2011). *Comput. Sci. Eng.* **13**, 22-30.

Wayman, C. M. (1964). *Introduction to the crystallography of martensitic transformations*. New York:
    MacMillan.

Wechsler, M. S., Lieberman, D. S. & Read, T. A. (1953). *A.I.M.E Trans* **197**, 1503-1515.

Yang, X.-P. & Zhang, W.-Z. (2012). *Sci. China Technol.Sci.***55**, 1343-1352.

Ye, F. & Zhang, W. Z. (2002). *Acta Mater.* **50**, 2761-2777.

Zhang, M. X. & Kelly, P. M. (2009). *Prog. Mater. Sci.***54**, 1101-1170.

Zhang, W.-Z. (2013). *Metall. Mater.Trans.* **44A**, 4513-4531.

Zhang, W.-Z. (2005). *Appl.Phys.Lett.* **86**, 121919.

Zhang, W.-Z. & Purdy, G. R. (1993). *Philos.Mag.* **68**, 291-303.

Zhang, W.-Z. & Weatherly, G. C. (2005). *Prog. Mater. Sci.***50**, 181-292.